AlGaN/GaN high-electron-mobility transistors with transparent gates by Al-doped ZnO*

Wang Chong(王 冲)[a)b)†], He Yun-Long(何云龙)[a)b)], Zheng Xue-Feng(郑雪峰)[a)b)], Ma Xiao-Hua(马晓华)[a)b)], Zhang Jin-Cheng(张进成)[a)b)], and Hao Yue(郝 跃)[a)b)]

[a)] *Key Laboratory of Wide Band Gap Semiconductor Materials and Devices, Xi'an* 710071, *China*
[b)] *The Institute of Microelectronics, Xidian University, Xi'an* 710071, *China*

(Received 21 September 2012; revised manuscript received 5 December 2012)

AlGaN/GaN high-electron-mobility transistors (HEMTs) with Al-doped ZnO (AZO) transparent gate electrodes are fabricated, and Ni/Au/Ni-gated HEMTs are produced in comparison. The AZO-gated HEMTs show good DC characteristics and Schottky rectifying characteristics, and the gate electrodes achieve excellent transparencies. Compared with Ni/Au/Ni-gated HEMTs, AZO-gated HEMTs show a low saturation current, high threshold voltage, high Schottky barrier height, and low gate reverse leakage current. Due to the higher gate resistivity, AZO-gated HEMTs exhibit a current–gain cutoff frequency (f_T) of 10 GHz and a power gain cutoff frequency (f_{max}) of 5 GHz, and lower maximum oscillation frequency than Ni/Au/Ni-gated HEMTs. Moreover, the *C*–*V* characteristics are measured and the gate interface characteristics of the AZO-gated devices are investigated by a *C*–*V* dual sweep.

Keywords: AlGaN/GaN, high-electron-mobility transistor, Al-doped ZnO

PACS: 85.30.Tv, 85.30.De, 85.35.Be **DOI:** 10.1088/1674-1056/22/6/068503

1. Introduction

AlGaN/GaN heterostructure high-electron-mobility transistors (HEMTs) are being actively pursued for high-power and high-frequency applications.[1] Their applications will also gradually extend to transparent electronics and terahertz detection.[2] However, these applications need to solve the problem of the transparent electrodes of AlGaN/GaN HEMTs.[3] High-performance optoelectronic devices receive a great deal of attention. Currently, the optoelectronic integrated circuit (OEIC) has become a research focus, and the combination of optoelectronic materials and electronic devices has become a trend.[4] With the development in photoelectric information technology, it is possible to study the defects and impurities using optical devices.[5] Pei *et al.*[6] reported on the technique to study the device characteristics for AlGaN/GaN HEMTs by using indium tin metal oxide (ITO) as the Schottky contact. Compared with ITO, AZO has attracted more attention in recent years due to its low cost, low resistivity, high transparency in the visible wavelength range, non-toxicity and stability under a hydrogen plasma environment.[7–9] Lee and Chou[10] reported on transparent AlGaAs/GaAs HEMTs by using AZO as the gate electrode.

In this paper, AZO-gated AlGaN/GaN HEMTs and Ni/Au/Ni-gated AlGaN/GaN HEMTs are fabricated. The DC characteristics, small signal characteristics, and the *C*–*V* characteristics of the AZO-gated HEMTs and Ni/Au/Ni-gated HEMTs are studied, respectively. To the best of the authors' knowledge, this paper is the first report dealing with GaN HEMTs with AZO gates.

2. Device fabrication

The AlGaN/GaN HEMT used in this paper was grown on a (0001) sapphire substrate in a metal organic chemical vapor deposition (MOCVD) system. The HEMT structure consists of a low-temperature GaN nucleation layer, a 1.8-μm thick unintentionally doped GaN buffer layer, a 16-nm undoped AlGaN barrier layer, and a thin undoped GaN cap layer. Room-temperature Hall measurements of the structure yielded an electron sheet density of 1.2×10^{13} cm^{-2} and an electron mobility of 1436 cm^2/V·s. Figure 1 shows a schematic diagram of the AZO-gated HEMTs and Ni/Au/Ni-gated HEMTs under study in this paper.

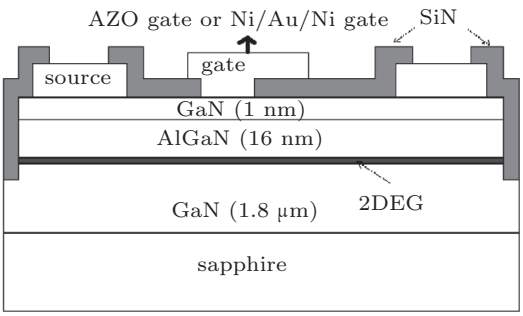


Fig. 1. Schematic plot of the studied AZO-gated HEMTs and Ni/Au/Ni-gated HEMTs.

*Project supported by the National Key Science & Technology Special Project (Grant No. 2008ZX01002-002), the National Natural Science Foundation of China (Grant No. 61106106), and the Fundamental Research Funds for the Central Universities, China (Grant Nos. K50510250003 and K50510250006).

†Corresponding author. E-mail: wangchong197810@hotmail.com

© 2013 Chinese Physical Society and IOP Publishing Ltd

Apart from the different gate material deposition technology, the two HEMTs had the same device processes. A device mesa was formed using Cl_2/Ar plasma dry etching in a reactive ion etching (RIE) system, followed by source/drain Ohmic contact formation with Ti/Al/Ni/Au annealed at 850 °C for 30 s. After SiN deposition of 60 nm on the surface of the devices by plasma-enhanced chemical vapor deposition (PECVD), the recessed-gate area was treated by CF_4 plasma in an RIE system at a radio frequency (RF) plasma bias voltage of 50 V. The gate recess was etched with a depth of 60 nm and width of 0.5 μm, and the gate material deposition and liftoff were carried out simultaneously to form the gate electrode. Ni/Au/Ni was used as the gate electrode of the conventional HEMT. The transparent gate electrode was deposited using a pulsed laser deposition (PLD) system at optimal deposition conditions. The wavelength of the KrF excimer pulsed laser, the energy, frequency, distance from the target material to the substrate, and the deposition temperature were 248 nm, 2 J/cm^2, 5 Hz, 55 mm, and 100 °C, respectively. The deposition process was in an O_2 environment. The pressure of the chamber, the background vacuum degree, and the thickness of the AZO film were 0.5 Pa, 1×10^{-4} Pa, and 210 nm, respectively. Both types of device have the same gate width of 100 μm, gate length of 0.5 μm, and source–drain space of 4 μm. In order to compare the different gate electrodes clearly, large-sized gate electrode devices, named FAT-FET, were also produced. The gate length, gate width, and source–drain space were 50 μm, 100 μm, and 56 μm, respectively. Figures 2(a) and 2(b) show the Ni/Au/Ni-gated and AZO-gated HEMTs, respectively, and a better transparency characteristic was observed in the AZO gate electrode. The device parameters were measured using the Keithley 4200 semiconductor parameter analyzer and the Agilent E8363 network analyzer. In this paper, all the results and curves are based on normal-sized devices.

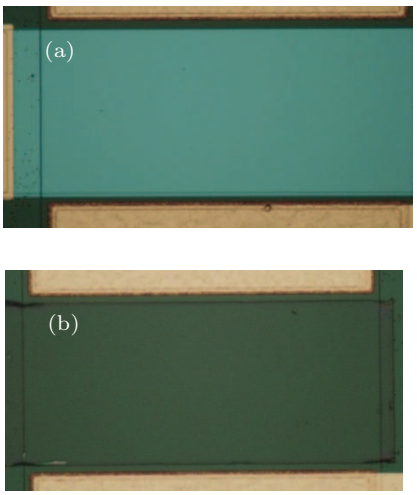


Fig. 2. (color online) The different gate electrodes of the FAT-FETs: Ni/Au/Ni-gated HEMT (a), and AZO-gated HEMT (b).

3. Device performance

The transfer characteristics and the transconductance characteristics of the AZO-gated HEMTs and Ni/Au/Ni-gated HEMTs are shown in Fig. 3. Compared with the Ni/Au/Ni-gated HEMT, the AZO-gated HEMT exhibits a small saturation current, high threshold voltage, and little difference in peak transconductance. The threshold voltage formula can be expressed as follows:[11]

$$V_{\rm th} = \frac{\phi_{\rm B}}{q} - \frac{\Delta E_{\rm c}}{q} - \frac{n_{\rm 2DEG} d}{\varepsilon}, \tag{1}$$

where $\Phi_{\rm B}$ is the Schottky barrier height, q the electronic charge, ε the dielectric constant of the semiconductor, d the distance from the gate to the two-dimensional electron gas (2DEG) channel, $\Delta E_{\rm c}$ the heterojunction conduction band discontinuity, and $n_{\rm 2DEG}$ the concentration of 2DEG. From Eq. (1), a lower 2DEG concentration and higher Schottky barrier height cause the threshold voltage to drift toward the positive direction of the x axis. The formation of the AZO gate electrode was implemented in an oxygen environment. Therefore, it is possible that a small amount of oxide layer was formed at the surface of the gate area, which could reduce the concentration of the 2DEG in the channel, so the maximum saturation current decreased slightly. Figure 4 shows the Schottky forward characteristic curves of the two devices. The height of the Schottky barrier of the AZO-gated HEMT is 0.87 eV, and that for the Ni/Au/Ni-gated HEMT is 0.72 eV. The ideality factor of the AZO-gated HEMT is 2.25, and that for the Ni/Au/Ni-gated device is 2.11. The higher barrier height of the AZO-gated HEMT yielded a stronger gate depletion, which causes the threshold voltage to drift toward the positive value direction.

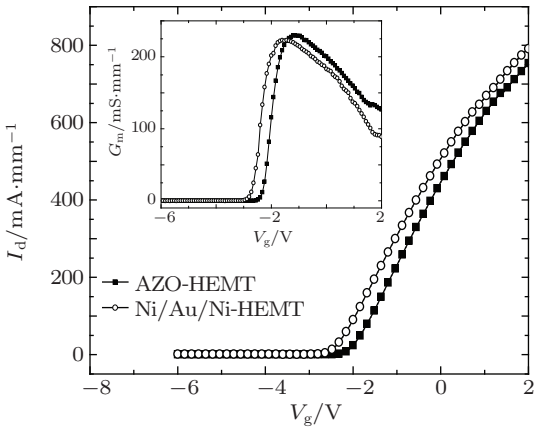


Fig. 3. Plots of the transfer characteristic and transconductance for the AZO-HEMT and the Ni/Au/Ni-HEMT.

The deposition of the AZO thin film can introduce surface damage and surface oxidation in an oxygen environment, which then causes a larger ideality factor of the AZO-gated HEMT. It was reported in some papers that the AZO-gated Schottky barrier height is lower than that of the Ni/Au/Ni

gate.[12] Our calculated barrier height of the AZO-gated device is larger than that given in other reports due to ignored series resistance in our calculation. Meanwhile, the barrier height is related to the AZO material, surface treatment process, and the Schottky barrier production process.

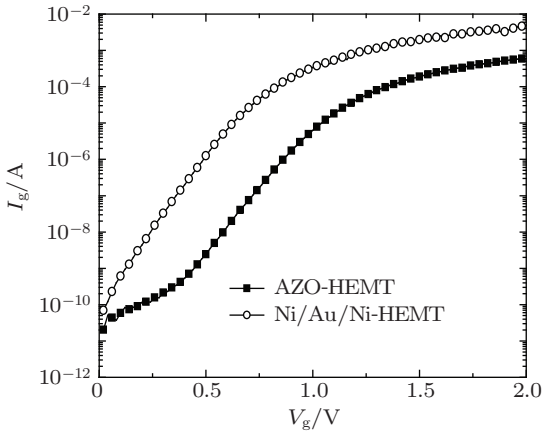


Fig. 4. Plots of Schottky forward characteristics for the AZO-HEMT and the Ni/Au/Ni-HEMT.

The Schottky reverse characteristics of the AZO-gated HEMT and the Ni/Au/Ni-gated HEMT are shown in Fig. 5. Compared with the Ni/Au/Ni-gated HEMT, the AZO-gated HEMT has a significant decrease in gate leakage current. On the one hand, the probability of electrons passing through the barrier are reduced due to the higher barrier height of the AZO-gated HEMT, which causes a certain inhibitory effect on the gate reverse leakage current; and on the other hand, the process of the AZO gate electrode may introduce an oxide layer, and the oxide layer can block the carriers as a dielectric, so the reverse leakage current is reduced.[13]

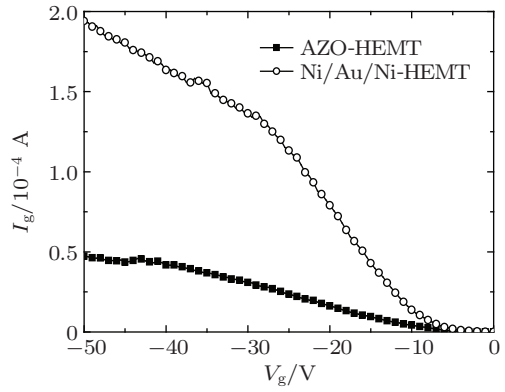


Fig. 5. Schottky reverse characteristics for the AZO-HEMT and the Ni/Au/Ni-HEMT.

The small signal measurement results of the AZO-gated HEMT are shown in Fig. 6. A current gain cutoff frequency (f_T) of 10 GHz and power gain cutoff frequency (f_{max}) of 5 GHz are achieved. Compared with the AZO-gated HEMT, the Ni/Au/Ni-gated HEMT has an f_T of 15 GHz and f_{max} of 40 GHz. The f_T and f_{max} of the AZO-gated HEMT are less than those of the Ni/Au/Ni-gated HEMT. The f_T could be influenced by the capacitance effect of the AZO gate. The AZO resistivity is about 2×10^{-4} Ω·cm, obtained by four-probe measurement, and that of Ni/Au/Ni is about 1×10^{-6} Ω·cm. As shown in formula (2), the gate resistance has a great influence on f_{max}. The small f_{max} of the AZO-gated HEMT is attributed to the larger gate resistance. The formula of f_{max} is

$$f_{max} \approx \sqrt{\frac{f_T}{8\pi R_g C_{gd}}}, \tag{2}$$

where R_G is the resistance of the gate, and C_{gd} the capacitance of the gate and drain.

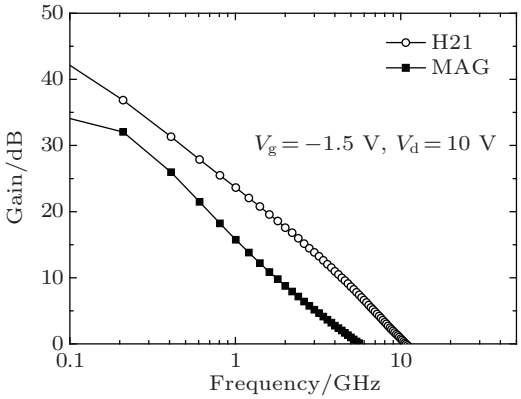


Fig. 6. The small signal characteristics for AZO-HEMT.

The relationship between the carrier concentration and the *C*–*V* curve can be expressed as

$$N_d = \frac{1}{\varepsilon\varepsilon_0 A^2} \times \frac{1}{dC^{-2}/dV}, \tag{3}$$

where N_d is the carrier concentration, A is the Schottky contact area, and ε and ε_0 are the dielectric constants of the air and the AlGaN, respectively. The frequency comparison between the *C*–*V* curves of the AZO-gated HEMT and the Ni/Au/Ni-gated HEMT is shown in Fig. 7. From formula (3), the 2DEG concentration is greatly related to the voltage applied to the Schottky barrier. The pinch-off voltage in the *C*–*V* curve of the AZO-gated HEMT is about 2.5 V, and that of the Ni/Au/Ni-gated HEMT is about 3 V. The pinch-off voltage in the *C*–*V* curve is dominated by the 2DEG concentration, which is related to the threshold voltage of the device.[14,15] Compared with the Ni/Au/Ni-gated HEMT, the AZO-gated HEMT has a small capacitance platform value with 1 MHz frequency, indicating that a series capacitance is induced by the AZO gate electrode at high frequency. When the frequency changes from 1 MHz to 100 kHz, no obvious change is found in the *C*–*V* curve.

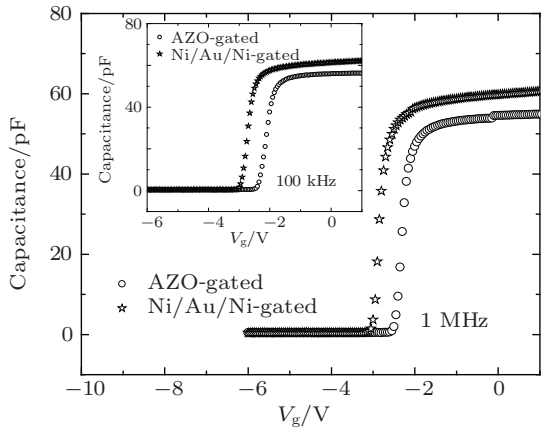


Fig. 7. The *C*–*V* characteristics at 1 MHz and 100 kHz for the AZO-HEMT and the Ni/Au/Ni-HEMT.

Figure 8 shows the *C*–*V* dual sweep curves of the AZO-gate device at frequencies of 100 kHz and 1 MHz. Under the 100 kHz frequency condition, the two curves coincide substantially, and under the 1 MHz frequency condition, the curves show a certain hysteresis, which is attributed to the bound electron in the traps under the gate at high frequency.[16,17]

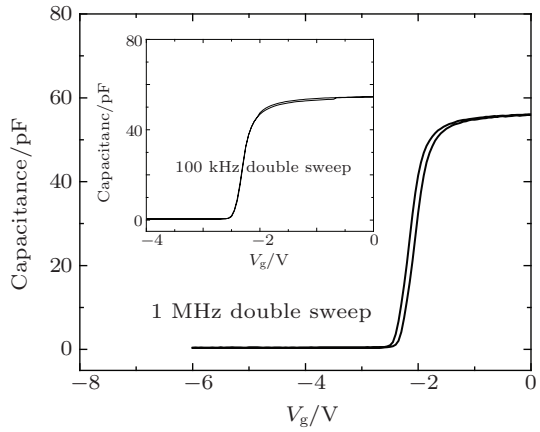


Fig. 8. The *C*–*V* dual sweep characteristics at 1 M and 100 kHz for the AZO-HEMT.

4. Conclusion

AZO-gated HEMTs were successfully fabricated, and the DC and small signal results are analyzed. Compared with the Ni/Au/Ni-gate HEMT, the AZO-gated HEMT shows a small saturation current, high threshold voltage, high Schottky barrier height, and small gate reverse leakage current. The AZO-gated HEMT exhibits an f_T of 10 GHz and f_{max} of 5 GHz. The poor f_{max} is due to the higher gate resistivity of the AZO-gated HEMT. The *C*–*V* characteristics are measured, and the AZO-gated device shows a lower platform value of capacitance, which is to a certain extent due to the series capacitance induced by the AZO gate electrode. The interface electron traps of the AZO-gated HEMTs are confirmed by the *C*–*V* dual sweep curves.

References

[1] Masataka H, Toshiaki M and Takashi M 2006 *IEEE Electron. Dev. Lett.* **27** 16

[2] Sun Y F, Sun J D, Zhang X Y, Qin H, Zhang B S and Wu D M 2012 *Chin. Phys. B* **21** 108504

[3] Wager J F 2003 *Science* **300** 1245

[4] Fan C, Chen T S, Yang L J, Feng O, Jiao S L, Wu Y F and Ye Y T 2009 *J. Semicond.* **30** 105009

[5] Meneghini M, Ronchi N, Stocco A, Meneghesso G, Mishra U K, Pei Y and Zanoni E 2011 *IEEE T. Electron. Dev.* **58** 2996

[6] Pei Y, Vampola K J, Chen Z, Chu R M, DenBaars S P and Mishra U K 2009 *IEEE Electron. Dev. Lett.* **30** 439

[7] Kim D C, Jung B O, Kwon Y H and Cho H K 2011 *J. Electrochem. Soc.* **159** 10

[8] Dong B Z, Hu H, Fang G J, Zhao X Z, Zheng D Y and Sun Y P 2008 *J. Appl. Phys.* **103** 073711

[9] Chen Z Q, Liu H M, Liu Y P, Chen W, Luo Z Q and Hu X W 2009 *Acta Phys. Sin.* **58** 4260 (in Chinese)

[10] Lee C S, Chou B Y and Hsu W C 2011 *IEEE Trans. Electron. Dev.* **58** 725

[11] Mahajan A, Arafa M, Fay P, Caneau C and Aesida I 1997 *IEEE Trans. Electron. Dev.* **18** 284

[12] Lee C S and Chou B Y 2010 *Electrochem. Solid-State Lett.* **13** 58

[13] Selvaraj S L, Ito T, Terada Y and Egawa T 2007 *Appl. Phys. Lett.* **90** 173506

[14] Wang C, Feng Q, Hao Y and Wan H 2006 *Acta Phys. Sin.* **55** 6085 (in Chinese)

[15] Zhou Y G, Shen B, Yu H Q, Liu J, Zhou H M, Zhang R, Shi Y, Zheng Y D, Someya T and Arakawa Y 2002 *Chin. Phys. Lett.* **19** 1172

[16] Chappel D C, Smith J P, Taylor S, Eccleston W, Das M K, Cooper J A and Melloch M R 1997 *Electron. Lett.* **33** 97

[17] Feng Q, Tian Y, Bi Z W, Yue Y Z, Ni J Y, Zhang J C, Hao Y and Yang L A 2009 *Chin. Phys. B* **18** 3014